

Fermi National Accelerator Laboratory

FERMILAB-Pub-97/283-E

CDF

**Dijet Production by Color-Singlet Exchange
at the Fermilab Tevatron**

F. Abe et al.

The CDF Collaboration

*Fermi National Accelerator Laboratory
P.O. Box 500, Batavia, Illinois 60510*

August 1997

Submitted to *Physical Review Letters*

Disclaimer

This report was prepared as an account of work sponsored by an agency of the United States Government. Neither the United States Government nor any agency thereof, nor any of their employees, makes any warranty, expressed or implied, or assumes any legal liability or responsibility for the accuracy, completeness, or usefulness of any information, apparatus, product, or process disclosed, or represents that its use would not infringe privately owned rights. Reference herein to any specific commercial product, process, or service by trade name, trademark, manufacturer, or otherwise, does not necessarily constitute or imply its endorsement, recommendation, or favoring by the United States Government or any agency thereof. The views and opinions of authors expressed herein do not necessarily state or reflect those of the United States Government or any agency thereof.

Distribution

Approved for public release; further dissemination unlimited.

Dijet Production by Color-Singlet Exchange at the Fermilab Tevatron

F. Abe,¹⁷ H. Akimoto,³⁸ A. Akopian,³¹ M. G. Albrow,⁷ S. R. Amendolia,²⁷ D. Amidei,²⁰
J. Antos,³³ S. Aota,³⁶ G. Apollinari,³¹ T. Arisawa,³⁸ T. Asakawa,³⁶ W. Ashmanskas,¹⁸
M. Atac,⁷ F. Azfar,²⁶ P. Azzi-Bacchetta,²⁵ N. Bacchetta,²⁵ W. Badgett,²⁰ S. Bagdasarov,³¹
M. W. Bailey,²² J. Bao,⁴⁰ P. de Barbaro,³⁰ A. Barbaro-Galtieri,¹⁸ V. E. Barnes,²⁹
B. A. Barnett,¹⁵ M. Barone,⁹ E. Barzi,⁹ G. Bauer,¹⁹ T. Baumann,¹¹ F. Bedeschi,²⁷
S. Behrends,³ S. Belforte,²⁷ G. Bellettini,²⁷ J. Bellinger,³⁹ D. Benjamin,³⁵ J. Benlloch,¹⁹
J. Bensinger,³ D. Benton,²⁶ A. Beretvas,⁷ J. P. Berge,⁷ J. Berryhill,⁵ S. Bertolucci,⁹
S. Bettelli,²⁷ B. Bevensee,²⁶ A. Bhatti,³¹ K. Biery,⁷ M. Binkley,⁷ D. Bisello,²⁵ R. E. Blair,¹
C. Blocker,³ S. Blusk,³⁰ A. Bodek,³⁰ W. Bokhari,²⁶ G. Bolla,²⁹ V. Bolognesi,² Y. Bonushkin,⁴
D. Bortoletto,²⁹ J. Boudreau,²⁸ L. Breccia,² C. Bromberg,²¹ N. Bruner,²² E. Buckley-Geer,⁷
H. S. Budd,³⁰ K. Burkett,²⁰ G. Busetto,²⁵ A. Byon-Wagner,⁷ K. L. Byrum,¹ C. Campagnari,⁷
M. Campbell,²⁰ A. Caner,²⁷ W. Carithers,¹⁸ D. Carlsmith,³⁹ J. Cassada,³⁰ A. Castro,²⁵
D. Cauz,²⁷ Y. Cen,³⁰ A. Cerri,²⁷ F. Cervelli,²⁷ P. S. Chang,³³ P. T. Chang,³³ H. Y. Chao,³³
J. Chapman,²⁰ M. -T. Cheng,³³ M. Chertok,³⁴ G. Chiarelli,²⁷ T. Chikamatsu,³⁶ C. N. Chiou,³³
L. Christofek,¹³ S. Cihangir,⁷ A. G. Clark,¹⁰ M. Cobal,²⁷ E. Cocca,²⁷ M. Contreras,⁵
J. Conway,³² J. Cooper,⁷ M. Cordelli,⁹ C. Couyoumtzelis,¹⁰ D. Crane,¹ D. Cronin-Hennessy,⁶
R. Culbertson,⁵ T. Daniels,¹⁹ F. DeJongh,⁷ S. Delchamps,⁷ S. Dell'Agnello,²⁷ M. Dell'Orso,²⁷
R. Demina,⁷ L. Demortier,³¹ M. Deninno,² P. F. Derwent,⁷ T. Devlin,³² J. R. Dittmann,⁶
S. Donati,²⁷ J. Done,³⁴ T. Dorigo,²⁵ A. Dunn,²⁰ N. Eddy,²⁰ K. Einsweiler,¹⁸ J. E. Elias,⁷
R. Ely,¹⁸ E. Engels, Jr.,²⁸ D. Errede,¹³ S. Errede,¹³ Q. Fan,³⁰ G. Feild,⁴⁰ Z. Feng,¹⁵
C. Ferretti,²⁷ I. Fiori,² B. Flaughner,⁷ G. W. Foster,⁷ M. Franklin,¹¹ M. Frautschi,³⁵
J. Freeman,⁷ J. Friedman,¹⁹ H. Frisch,⁵ Y. Fukui,¹⁷ S. Funaki,³⁶ S. Galeotti,²⁷ M. Gallinaro,²⁶
O. Ganel,³⁵ M. Garcia-Sciveres,¹⁸ A. F. Garfinkel,²⁹ C. Gay,¹¹ S. Geer,⁷ D. W. Gerdes,¹⁵
P. Giannetti,²⁷ N. Giokaris,³¹ G. Giusti,²⁷ L. Gladney,²⁶ M. Gold,²² J. Gonzalez,²⁶

A. Gordon,¹¹ A. T. Goshaw,⁶ Y. Gotra,²⁵ K. Goulianos,³¹ H. Grassmann,²⁷ L. Groer,³²
C. Grosso-Pilcher,⁵ G. Guillian,²⁰ J. Guimarães,¹⁵ R. S. Guo,³³ C. Haber,¹⁸ E. Hafen,¹⁹
S. R. Hahn,⁷ R. Hamilton,¹¹ R. Handler,³⁹ R. M. Hans,⁴⁰ F. Happacher,⁹ K. Hara,³⁶
A. D. Hardman,²⁹ B. Harral,²⁶ R. M. Harris,⁷ S. A. Hauger,⁶ J. Hauser,⁴ C. Hawk,³²
E. Hayashi,³⁶ J. Heinrich,²⁶ B. Hinrichsen,¹⁴ K. D. Hoffman,²⁹ M. Hohlmann,⁵ C. Holck,²⁶
R. Hollebeek,²⁶ L. Holloway,¹³ S. Hong,²⁰ G. Houk,²⁶ P. Hu,²⁸ B. T. Huffman,²⁸ R. Hughes,²³
J. Huston,²¹ J. Huth,¹¹ J. Hysten,⁷ H. Ikeda,³⁶ M. Incagli,²⁷ J. Incandela,⁷ G. Introzzi,²⁷
J. Iwai,³⁸ Y. Iwata,¹² H. Jensen,⁷ U. Joshi,⁷ R. W. Kadel,¹⁸ E. Kajfasz,²⁵ H. Kambara,¹⁰
T. Kamon,³⁴ T. Kaneko,³⁶ K. Karr,³⁷ H. Kasha,⁴⁰ Y. Kato,²⁴ T. A. Keaffaber,²⁹ K. Kelley,¹⁹
R. D. Kennedy,⁷ R. Kephart,⁷ P. Kesten,¹⁸ D. Kestenbaum,¹¹ H. Keutelian,⁷ F. Keyvan,⁴
B. Kharadia,¹³ B. J. Kim,³⁰ D. H. Kim,^{7a} H. S. Kim,¹⁴ S. B. Kim,²⁰ S. H. Kim,³⁶
Y. K. Kim,¹⁸ L. Kirsch,³ P. Koehn,²³ A. Köngeter,¹⁶ K. Kondo,³⁶ J. Konigsberg,⁸ S. Kopp,⁵
K. Kordas,¹⁴ A. Korytov,⁸ W. Koska,⁷ E. Kovacs,^{7a} W. Kowald,⁶ M. Krasberg,²⁰ J. Kroll,⁷
M. Kruse,³⁰ S. E. Kuhlmann,¹ E. Kuns,³² T. Kuwabara,³⁶ A. T. Laasanen,²⁹ S. Lami,²⁷
S. Lammel,⁷ J. I. Lamoureux,³ M. Lancaster,¹⁸ M. Lanzoni,²⁷ G. Latino,²⁷ T. LeCompte,¹
S. Leone,²⁷ J. D. Lewis,⁷ P. Limon,⁷ M. Lindgren,⁴ T. M. Liss,¹³ J. B. Liu,³⁰ Y. C. Liu,³³
N. Lockyer,²⁶ O. Long,²⁶ C. Loomis,³² M. Loreti,²⁵ J. Lu,³⁴ D. Lucchesi,²⁷ P. Lukens,⁷
S. Lusin,³⁹ J. Lys,¹⁸ K. Maeshima,⁷ A. Maghakian,³¹ P. Maksimovic,¹⁹ M. Mangano,²⁷
M. Mariotti,²⁵ J. P. Marriner,⁷ A. Martin,⁴⁰ J. A. J. Matthews,²² R. Mattingly,¹⁹
P. Mazzanti,² P. McIntyre,³⁴ P. Melese,³¹ A. Menzione,²⁷ E. Meschi,²⁷ C. Mesropian,³¹
S. Metzler,²⁶ C. Miao,²⁰ T. Miao,⁷ G. Michail,¹¹ R. Miller,²¹ H. Minato,³⁶ S. Miscetti,⁹
M. Mishina,¹⁷ H. Mitsushio,³⁶ T. Miyamoto,³⁶ S. Miyashita,³⁶ N. Moggi,²⁷ Y. Morita,¹⁷
A. Mukherjee,⁷ T. Muller,¹⁶ P. Murat,²⁷ S. Murgia,²¹ H. Nakada,³⁶ I. Nakano,³⁶ C. Nelson,⁷
D. Neuberger,¹⁶ C. Newman-Holmes,⁷ C.-Y. P. Ngan,¹⁹ M. Ninomiya,³⁶ L. Nodulman,¹
S. H. Oh,⁶ K. E. Ohl,⁴⁰ T. Ohmoto,¹² T. Ohsugi,¹² R. Oishi,³⁶ M. Okabe,³⁶ T. Okusawa,²⁴
R. Oliveira,²⁶ J. Olsen,³⁹ C. Pagliarone,²⁷ R. Paoletti,²⁷ V. Papadimitriou,³⁵ S. P. Pappas,⁴⁰
N. Parashar,²⁷ S. Park,⁷ A. Parri,⁹ J. Patrick,⁷ G. Pauletta,²⁷ M. Paulini,¹⁸ A. Perazzo,²⁷
L. Pescara,²⁵ M. D. Peters,¹⁸ T. J. Phillips,⁶ G. Piacentino,²⁷ M. Pillai,³⁰ K. T. Pitts,⁷

R. Plunkett,⁷ L. Pondrom,³⁹ J. Proudfoot,¹ F. Ptohos,¹¹ G. Punzi,²⁷ K. Ragan,¹⁴ D. Reher,¹⁸
A. Ribon,²⁵ F. Rimondi,² L. Ristori,²⁷ W. J. Robertson,⁶ T. Rodrigo,²⁷ S. Rolli,³⁷
J. Romano,⁵ L. Rosenson,¹⁹ R. Roser,¹³ T. Saab,¹⁴ W. K. Sakumoto,³⁰ D. Saltzberg,⁴
A. Sansoni,⁹ L. Santi,²⁷ H. Sato,³⁶ P. Schlabach,⁷ E. E. Schmidt,⁷ M. P. Schmidt,⁴⁰ A. Scott,⁴
A. Scribano,²⁷ S. Segler,⁷ S. Seidel,²² Y. Seiya,³⁶ F. Semeria,² G. Sganos,¹⁴ T. Shah,¹⁹
M. D. Shapiro,¹⁸ N. M. Shaw,²⁹ Q. Shen,²⁹ P. F. Shepard,²⁸ M. Shimojima,³⁶ M. Shochet,⁵
J. Siegrist,¹⁸ A. Sill,³⁵ P. Sinervo,¹⁴ P. Singh,¹³ K. Sliwa,³⁷ C. Smith,¹⁵ F. D. Snider,¹⁵
T. Song,²⁰ J. Spalding,⁷ T. Speer,¹⁰ P. Sphicas,¹⁹ F. Spinella,²⁷ M. Spiropulu,¹¹ L. Spiegel,⁷
L. Stanco,²⁵ J. Steele,³⁹ A. Stefanini,²⁷ J. Strait,⁷ R. Ströhmer,^{7a} D. Stuart,⁷ G. Sullivan,⁵
K. Sumorok,¹⁹ J. Suzuki,³⁶ T. Takada,³⁶ T. Takahashi,²⁴ T. Takano,³⁶ K. Takikawa,³⁶
N. Tamura,¹² B. Tannenbaum,²² F. Tartarelli,²⁷ W. Taylor,¹⁴ P. K. Teng,³³ Y. Teramoto,²⁴
S. Tether,¹⁹ D. Theriot,⁷ T. L. Thomas,²² R. Thun,²⁰ R. Thurman-Keup,¹ M. Timko,³⁷
P. Tipton,³⁰ A. Titov,³¹ S. Tkaczyk,⁷ D. Toback,⁵ K. Tollefson,³⁰ A. Tollestrup,⁷ H. Toyoda,²⁴
W. Trischuk,¹⁴ J. F. de Troconiz,¹¹ S. Truitt,²⁰ J. Tseng,¹⁹ N. Turini,²⁷ T. Uchida,³⁶
N. Uemura,³⁶ F. Ukegawa,²⁶ G. Unal,²⁶ J. Valls,^{7a} S. C. van den Brink,²⁸ S. Vejckic,
III,²⁰ G. Velev,²⁷ R. Vidal,⁷ R. Vilar,^{7a} M. Vondracek,¹³ D. Vucinic,¹⁹ R. G. Wagner,¹
R. L. Wagner,⁷ J. Wahl,⁵ N. B. Wallace,²⁷ A. M. Walsh,³² C. Wang,⁶ C. H. Wang,³³
J. Wang,⁵ M. J. Wang,³³ Q. F. Wang,³¹ A. Warburton,¹⁴ T. Watts,³² R. Webb,³⁴ C. Wei,⁶
H. Wei,³⁵ H. Wenzel,¹⁶ W. C. Wester, III,⁷ A. B. Wicklund,¹ E. Wicklund,⁷ R. Wilkinson,²⁶
H. H. Williams,²⁶ P. Wilson,⁵ B. L. Winer,²³ D. Winn,²⁰ D. Wolinski,²⁰ J. Wolinski,²¹
S. Worm,²² X. Wu,¹⁰ J. Wyss,²⁵ A. Yagil,⁷ W. Yao,¹⁸ K. Yasuoka,³⁶ Y. Ye,¹⁴ G. P. Yeh,⁷
P. Yeh,³³ M. Yin,⁶ J. Yoh,⁷ C. Yosef,²¹ T. Yoshida,²⁴ D. Yovanovitch,⁷ I. Yu,⁷ L. Yu,²²
J. C. Yun,⁷ A. Zanetti,²⁷ F. Zetti,²⁷ L. Zhang,³⁹ W. Zhang,²⁶ and S. Zucchelli²

(CDF Collaboration)

¹ Argonne National Laboratory, Argonne, Illinois 60439

² Istituto Nazionale di Fisica Nucleare, University of Bologna, I-40127 Bologna, Italy

- ³ *Brandeis University, Waltham, Massachusetts 02254*
- ⁴ *University of California at Los Angeles, Los Angeles, California 90024*
- ⁵ *University of Chicago, Chicago, Illinois 60637*
- ⁶ *Duke University, Durham, North Carolina 27708*
- ⁷ *Fermi National Accelerator Laboratory, Batavia, Illinois 60510*
- ⁸ *University of Florida, Gainesville, FL 32611*
- ⁹ *Laboratori Nazionali di Frascati, Istituto Nazionale di Fisica Nucleare, I-00044 Frascati, Italy*
- ¹⁰ *University of Geneva, CH-1211 Geneva 4, Switzerland*
- ¹¹ *Harvard University, Cambridge, Massachusetts 02138*
- ¹² *Hiroshima University, Higashi-Hiroshima 724, Japan*
- ¹³ *University of Illinois, Urbana, Illinois 61801*
- ¹⁴ *Institute of Particle Physics, McGill University, Montreal H3A 2T8, and University of Toronto,
Toronto M5S 1A7, Canada*
- ¹⁵ *The Johns Hopkins University, Baltimore, Maryland 21218*
- ¹⁶ *Institut für Experimentelle Kernphysik, Universität Karlsruhe, 76128 Karlsruhe, Germany*
- ¹⁷ *National Laboratory for High Energy Physics (KEK), Tsukuba, Ibaraki 315, Japan*
- ¹⁸ *Ernest Orlando Lawrence Berkeley National Laboratory, Berkeley, California 94720*
- ¹⁹ *Massachusetts Institute of Technology, Cambridge, Massachusetts 02139*
- ²⁰ *University of Michigan, Ann Arbor, Michigan 48109*
- ²¹ *Michigan State University, East Lansing, Michigan 48824*
- ²² *University of New Mexico, Albuquerque, New Mexico 87131*
- ²³ *The Ohio State University, Columbus, OH 43210*
- ²⁴ *Osaka City University, Osaka 588, Japan*
- ²⁵ *Università di Padova, Istituto Nazionale di Fisica Nucleare, Sezione di Padova, I-36132 Padova, Italy*
- ²⁶ *University of Pennsylvania, Philadelphia, Pennsylvania 19104*
- ²⁷ *Istituto Nazionale di Fisica Nucleare, University and Scuola Normale Superiore of Pisa, I-56100 Pisa, Italy*
- ²⁸ *University of Pittsburgh, Pittsburgh, Pennsylvania 15260*
- ²⁹ *Purdue University, West Lafayette, Indiana 47907*

- ³⁰ *University of Rochester, Rochester, New York 14627*
- ³¹ *Rockefeller University, New York, New York 10021*
- ³² *Rutgers University, Piscataway, New Jersey 08855*
- ³³ *Academia Sinica, Taipei, Taiwan 11530, Republic of China*
- ³⁴ *Texas A&M University, College Station, Texas 77843*
- ³⁵ *Texas Tech University, Lubbock, Texas 79409*
- ³⁶ *University of Tsukuba, Tsukuba, Ibaraki 315, Japan*
- ³⁷ *Tufts University, Medford, Massachusetts 02155*
- ³⁸ *Waseda University, Tokyo 169, Japan*
- ³⁹ *University of Wisconsin, Madison, Wisconsin 53706*
- ⁴⁰ *Yale University, New Haven, Connecticut 06520*

Abstract

We report a new measurement of dijet production by color-singlet exchange in $p\bar{p}$ collisions at $\sqrt{s} = 1.8$ TeV at the Fermilab Tevatron, and present results on the dependence of the cross section on jet transverse energy and pseudorapidity separation between the jets. In a sample of events with two jets of transverse energy $E_T^{jet} > 20$ GeV, pseudorapidity in the range $1.8 < |\eta^{jet}| < 3.5$, and $\eta_1\eta_2 < 0$, we find that a fraction $R = 1.13 \pm 0.12(stat) \pm 0.11(syst)\%$ have a pseudorapidity gap within $|\eta| < 1$ between the jets that can be attributed to color-singlet exchange. The fraction R shows no significant dependence on E_T^{jet} or on the pseudorapidity separation between the jets.

PACS number(s): 13.87.Fh, 12.38.Qk, 13.85.Hd

Typeset using REVTeX

In high energy hadron collisions jets are usually produced through the exchange of a quark or gluon between partons of the interacting hadrons. Because of the net color flow associated with such an exchange, particles are commonly produced in the rapidity [1] region between the jets. However, jets may also be produced by a colorless exchange, such as strongly interacting color-singlet or electroweak boson (γ , W , Z^0) exchange, resulting in events with a “rapidity gap” between the jets, namely a region of rapidity devoid of particles. In a simple model of a two-gluon color-singlet exchange, the ratio of two-jet (dijet) events with a rapidity gap to all two-jet events produced in $\bar{p}p$ collisions at $\sqrt{s} = 1.8$ TeV was estimated to be $R \sim 10^{-2}$ [2,3] independent of rapidity gap width or jet transverse energy (E_T^{jet}); for electroweak exchange, R is expected to be $\sim 10^{-4}$ [3]. The production rate and characteristics of dijet events with a rapidity gap between jets can be used to probe the nature of the colorless exchange process.

The ratio R has been measured in $p\bar{p}$ collisions at $\sqrt{s} = 1.8$ TeV by the CDF [4] and DØ [5] Collaborations at the Fermilab Tevatron, and in photoproduction at a center of mass energy of ~ 150 GeV by the ZEUS Collaboration [6] at HERA. The reported values are $R_{\text{CDF}} = [0.85 \pm 0.12(stat)_{-0.12}^{+0.24}(syst)]\%$ for dijets with leading (highest E_T) jet $E_T > 40$ GeV and $|\Delta\eta| > 1.5$, $R_{\text{DØ}} = [1.07 \pm 0.10(stat)_{-0.13}^{+0.25}(syst)]\%$ for $E_T^{jet} > 30$ GeV, $|\eta^{jet}| > 2$ and $\eta_1\eta_2 < 0$, and $R_{\text{ZEUS}} \approx 7\%$ for jets of $E_T > 6$ GeV photoproduced at HERA. The magnitude of the measured ratio suggests that the dijet system is produced through strongly interacting color-singlet exchange. In all cases, the background rapidity gap fraction due to normal color-octet exchange was estimated by using Monte Carlo simulations and/or fits to the particle multiplicity distribution in the rapidity region between the jets. In this letter, we present a new measurement of R at the Tevatron based on a more direct method of background subtraction with different, and smaller, systematic uncertainties. We also present a study of some characteristics of a sample of rapidity gap events, such as third-jet activity and dependence of R on E_T^{jet} and on the rapidity interval between the jets.

The CDF detector is described in detail elsewhere [7]. The detector components relevant to this study are the Central Tracking Chamber (CTC), which detects charged particles,

and the calorimeters, which detect both charged and neutral particles. The CTC tracking efficiency varies from $\sim 60\%$ for $P_T = 300$ MeV to over 95% for $P_T > 400$ MeV within $|\eta| < 1.2$, falls monotonically beyond $|\eta| = 1.2$, and approaches zero at $|\eta| \sim 1.8$. The calorimeters have projective tower geometry and cover the regions $|\eta| < 1.1$ (central), $1.1 < |\eta| < 2.4$ (plug), and $2.2 < |\eta| < 4.2$ (forward). The $\Delta\eta \times \Delta\phi$ tower dimensions are $0.1 \times 15^\circ$ for the central and $0.1 \times 5^\circ$ for the plug and forward calorimeters. For this analysis, a “charged particle” is a reconstructed 3-dimensional track with $P_T > 300$ MeV. The “tower multiplicity” is defined as the number of calorimeter towers with measured $E_T > 200$ MeV, which corresponds approximately to true $E_T > 300$ MeV.

The data sample consists of events collected in a run of total integrated luminosity 2.2 pb^{-1} , using a trigger requiring two high E_T jets at $|\eta| > 1.4$. Because of the high instantaneous luminosity during data collection, a large fraction of the events had one or more additional (“minimum bias”) events superimposed on the dijet event that caused the trigger. Since an overlay of minimum bias events could obscure a rapidity gap, we selected a sub-sample of events with no more than one primary reconstructed vertex ($N_{\text{vertex}} \leq 1$) within ± 60 cm of the nominal interaction point. About 16% of the events passed this selection cut. After the jet E_T , defined as the sum of the calorimeter E_T within an $\eta - \phi$ cone of radius 0.7 , was corrected for non-linearities in the calorimeter response and for energy lost in uninstrumented regions, the two leading jets were required to have $E_T^{\text{jet}} > 20$ GeV and $1.8 < |\eta| < 3.5$. No requirement was imposed on additional jets in an event. The remaining dijet sample consists of 10200 events with the leading jets on opposite η -sides ($\eta_1\eta_2 < 0$), and 30352 events with both leading jets on the same η -side ($\eta_1\eta_2 > 0$). The same-side dijet event sample was used for the measurement of the production rate of diffractive dijet events presented in [8]. In this analysis, these events are used as a “control” sample in evaluating the color-octet contribution to events with a rapidity gap between jets in the opposite-side sample, as discussed below.

The distributions of the leading jet E_T and η , $E_T^{(1)}$ and η_1 , and of the differences $\Delta E_T = E_T^{(1)} - E_T^{(2)}$ and $\Delta\phi = \phi_1 - \phi_2$ for the two leading jets are shown in Fig. 1. The structure at

$|\eta| \sim 2.2 - 2.4$ is caused by the lower calorimetric response at the interface between different detector components. The two jets tend to be balanced both in E_T and ϕ . About 85% of the events contain a third jet of $E_T^{(3)} > 5$ GeV. The $E_T^{(3)}$ and η_3 distributions of the third jet are also shown in Fig. 1. The corresponding distributions of the same-side dijet sample are very similar [8].

Rapidity gaps between jets can occur naturally in color-octet exchange dijet events by fluctuations of the underlying soft particle multiplicity. We first search for rapidity gaps due to color-singlet exchange by analyzing the event track multiplicity, N_{track} , in the region $|\eta| < 1.0$. Figure 2(a) shows the multiplicity of tracks with $P_T > 300$ MeV within $|\eta| < 1.0$ for opposite-side (solid) and within $|\eta| < 1.2$ for same-side (dashed) dijet events. The η -range of the same-side distribution was chosen to yield the same mean multiplicity as the opposite-side distribution, and the normalization was scaled down by a factor $C = 0.34$, which is the ratio of opposite-side to same-side events with $N_{\text{track}} > 0$. Figure 2(c) shows the bin-by-bin asymmetry (difference over sum) of the two distributions shown in Fig. 2(a). The asymmetry is consistent with zero in all bins except in the zero-multiplicity bin. From a detailed analysis of the same-side data sample [8], we estimate that the contribution from single diffractive events in the $N_{\text{track}} = 0$ bin of the same-side sample is negligibly small. Thus, we use the number of events in the $N_{\text{track}} = 0$ bin of the same-side distribution as the expectation for opposite-side events due to color-octet exchange and attribute the excess above this number to color-singlet exchange. The fractional excess over all events is $R_1 = [2.06 \pm 0.22(\text{stat}) \pm 0.09(\text{syst})]\%$, where the systematic error reflects the uncertainty due to background subtraction and the subscript “1” refers to the $N_{\text{vertex}} \leq 1$ requirement.

A similar analysis was performed using the multiplicity of calorimeter towers with measured $E_T > 200$ MeV within $|\eta| < 1.0$ for opposite-side and $|\eta| < 1.25$ for same-side events. In Figs. 2(b,d), a clear excess is seen in opposite-side over same-side events in the bins $N_{\text{tower}}=0, 1$ and 2. The combined excess in these three bins yields a fraction of $[1.92 \pm 0.20(\text{stat})]\%$; incorporating the fourth bin yields $[2.21 \pm 0.25(\text{stat})]\%$. These values are consistent with the result obtained from the track multiplicity analysis. The spilling of

the rapidity gap signal into non-zero tower-multiplicity bins is mainly due to calorimeter noise, with some additional spreading resulting presumably from γ 's entering the gap region from the decay of parent neutral mesons produced within the jet regions. Because of the larger systematic uncertainties involved in the tower multiplicity analysis, we use the tracking result, R_1 , and correct it for the $N_{\text{vertex}} \leq 1$ efficiency, as discussed below, to obtain the fraction, R , for the total opposite-side event sample.

The $N_{\text{vertex}} \leq 1$ selection cut, which is used to reject events due to multiple interactions, also rejects single interaction dijet events with more than one *reconstructed* vertex. Extra vertices in a dijet event are due to confusion in reconstruction caused by the high particle multiplicity. The ratio R_1 must therefore be corrected for the efficiency (fraction of events retained) of this cut, which affects primarily the “non-gap” events, which have higher multiplicity in the central region. The efficiency for non-gap events was measured to be $0.55 \pm 0.05(\text{sys})$ by comparing the fraction of single vertex dijet events to all dijet events in a given run with the fraction expected from the instantaneous luminosity in the same time period. The assigned uncertainty is due to the variations found as a function of instantaneous luminosity. For “gap” events, the vertex selection efficiency was found to be $1.00^{+0.00}_{-0.03}$. Correcting R_1 for the vertex selection efficiency we obtain

$$R = [1.13 \pm 0.12(\text{stat}) \pm 0.11(\text{sys})]\%$$

This value is in good agreement with the published values of CDF [4] and DØ [5] and, as stated previously, its magnitude indicates that the dijet system is produced by strongly-interacting color-singlet exchange.

Figure 3 shows the correlation of towers versus tracks for opposite-side dijet events with $N_{\text{track}} < 5$ and $N_{\text{tower}} < 21$ within $|\eta| < 1.0$. The bins with $N_{\text{track}} = 0$ and $N_{\text{tower}} = 0, 1$ or 2 , in which the color-singlet exchange signal is expected to be concentrated, contain a total of 221 “gap” events. From an analysis based on a two-dimensional extrapolation from the nearby bins, we estimate that these 221 events contain 25% color-octet exchange background. For this reason, and as a check for possible detector biases, we present distributions of

kinematical variables of the gap events along with corresponding distributions of a “control” sample consisting of events with 1, 2 or 3 tracks and up to 6 towers. Figure 4 shows normalized ratios of gap and control sample events to all events as a function of the average E_T of the two leading jets, the E_T of the third jet, and the η -separation of the two leading jets. In each case, the total number of gap or control sample events is normalized to the number of “all events”. The gap and control samples behave similarly. The colorless exchange fraction is fairly independent of jet E_T and $\Delta\eta$, decreasing somewhat at large $\Delta\eta$.

In the two-gluon model of Ref. [2], the gap to non-gap ratio is predicted to be independent of jet E_T and $\Delta\eta$. Calculations [9] using a model [10] based on the Balitsky-Fadin-Kuraev-Lipatov (BFKL) [11] resummation of a color-singlet gluon ladder exchange also predict a “basically flat” [12] distribution of R versus $\Delta\eta$. Our results are in general agreement with these predictions, but further investigations with higher statistics are needed before firm conclusions can be drawn about the nature of the color-singlet exchange process.

In conclusion, we report a new measurement of the fraction of dijet events with a rapidity gap between jets in $p\bar{p}$ collisions at $\sqrt{s} = 1.8$ TeV and present the results of a study of rapidity-gap event characteristics. We find that for jets of $E_T^{jet} > 20$ GeV, pseudorapidity $1.8 < |\eta| < 3.5$ and $\eta_1\eta_2 < 0$, the fraction of events that can be attributed to color-singlet exchange is $1.13 \pm 0.12(stat) \pm 0.11(syst)\%$, in good agreement with previous measurements [4,5]. The rapidity-gap fraction is fairly independent of jet E_T within $25 < E_T < 55$ GeV and of the rapidity interval between the jets within $4 < \Delta\eta < 6$, decreasing somewhat at the largest values of $\Delta\eta$.

We thank the Fermilab staff and the technical staffs of the participating institutions for their vital contributions. This work was supported by the U.S. Department of Energy and National Science Foundation; the Italian Istituto Nazionale di Fisica Nucleare; the Ministry of Education, Science and Culture of Japan; the Natural Sciences and Engineering Research Council of Canada; the National Science Council of the Republic of China; and the A. P. Sloan Foundation.

REFERENCES

- [1] We use rapidity and pseudorapidity, η , interchangeably; $\eta \equiv -\ln(\tan\frac{\theta}{2})$, where θ is the polar angle of a particle with respect to the proton beam direction. The azimuthal angle is denoted by ϕ , and the transverse momentum (energy) of a (particle) jet, is defined as $P_T(E_T) = P(E) \sin \theta$.
- [2] J.D. Bjorken, Phys. Rev. **D47**, 101 (1993).
- [3] H. Chehime *et al.*, Phys. Lett. **B286**, 397 (1992).
- [4] F. Abe *et al.*, Phys. Rev. Lett. **74**, 855 (1995).
- [5] S. Abachi *et al.*, Phys. Rev. Lett. **76**, 734 (1996).
- [6] M. Derrick *et al.*, Phys. Lett. **B369**, 55 (1996).
- [7] F. Abe *et al.*, Nucl. Instrum. Methods **A271**, 387 (1988).
- [8] F. Abe *et al.*, “Measurement of Diffractive Dijet Production at the Fermilab Tevatron”, submitted to Phys. Rev. Letters.
- [9] V. Del Duca and W.-K. Tang, Phys. Lett. **B312**, 225 (1993).
- [10] A.H.Mueller and W.-K.Tang, Phys. Lett. **B284**, 123 (1992).
- [11] L. N. Lipatov, Sov. J. Nucl. Phys. **23**, 338 (1976); E. A. Kuraev, L. N. Lipatov and V. S. Fadin, Sov. Phys. JETP **44**, 443 (1976); Sov. Phys. JETP **45**, 199 (1977); Ya. Ya. Balitsky and L. N. Lipatov, Sov. J. Nucl. Phys. **28**, 822 (1978).
- [12] V. Del Duca, Proceedings of the 10th Topical Workshop on Proton-Antiproton Collider Physics, Fermilab, 9-13 May 1995.

FIGURES

FIG. 1. (*top*) Leading jet transverse energy and pseudorapidity (the structure at $|\eta| \sim 2.2 - 2.4$ is instrumental); (*middle*) difference between the transverse energies and azimuthal angles of the two leading jets; (*bottom*) third jet ($E_T^{(3)} > 5$ GeV) transverse energy and pseudorapidity.

FIG. 2. Multiplicity distributions (a) for tracks with $P_T > 300$ MeV and (b) for calorimeter towers with measured $E_T > 200$ MeV in the regions $|\eta| < 1.0$ for opposite-side ($\eta_1 \eta_2 < 0$) dijet events (solid lines), and $|\eta| < 1.2$ ($|\eta| < 1.25$) for tracks (towers) of same-side ($\eta_1 \eta_2 > 0$) dijet events (dashed lines); (c,d) The bin-by-bin asymmetry, defined as the ratio of the difference over the sum of the opposite-side and same-side multiplicity distributions of (a) and (b).

FIG. 3. Track versus tower multiplicity distribution for events in the $N_{\text{vertex}} \leq 1$ opposite-side dijet sample with $N_{\text{track}} < 5$ and $N_{\text{tower}} < 21$ within $|\eta| < 1.0$. The bins with zero tracks and 0, 1 or 2 towers contain an excess of events above the expectation from an extrapolation from the bins with $N_{\text{track}} > 1$. This excess is attributed to events from color-singlet exchange.

FIG. 4. Normalized (to be unity on average) ratios of gap (solid points) and control sample events (open circles) over all events versus: (a) the average E_T of the two leading jets, (b) the E_T of the third jet, and (c) half the η separation between the two leading jets.

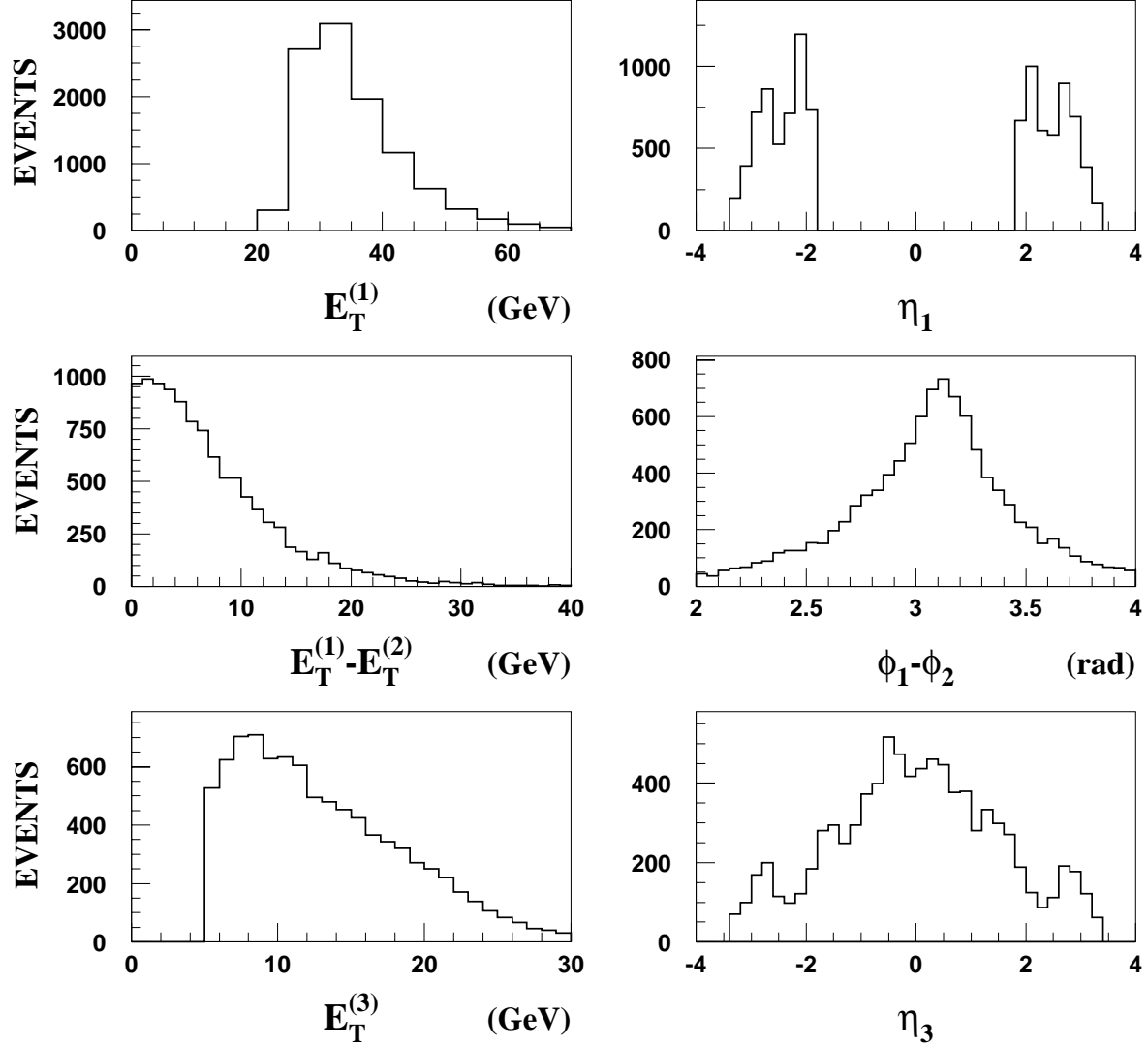


FIG. 1. (*top*) Leading jet transverse energy and pseudorapidity (the structure at $|\eta| \sim 2.2 - 2.4$ is instrumental); (*middle*) difference between the transverse energies and azimuthal angles of the two leading jets; (*bottom*) third jet ($E_T^{(3)} > 5$ GeV) transverse energy and pseudorapidity.

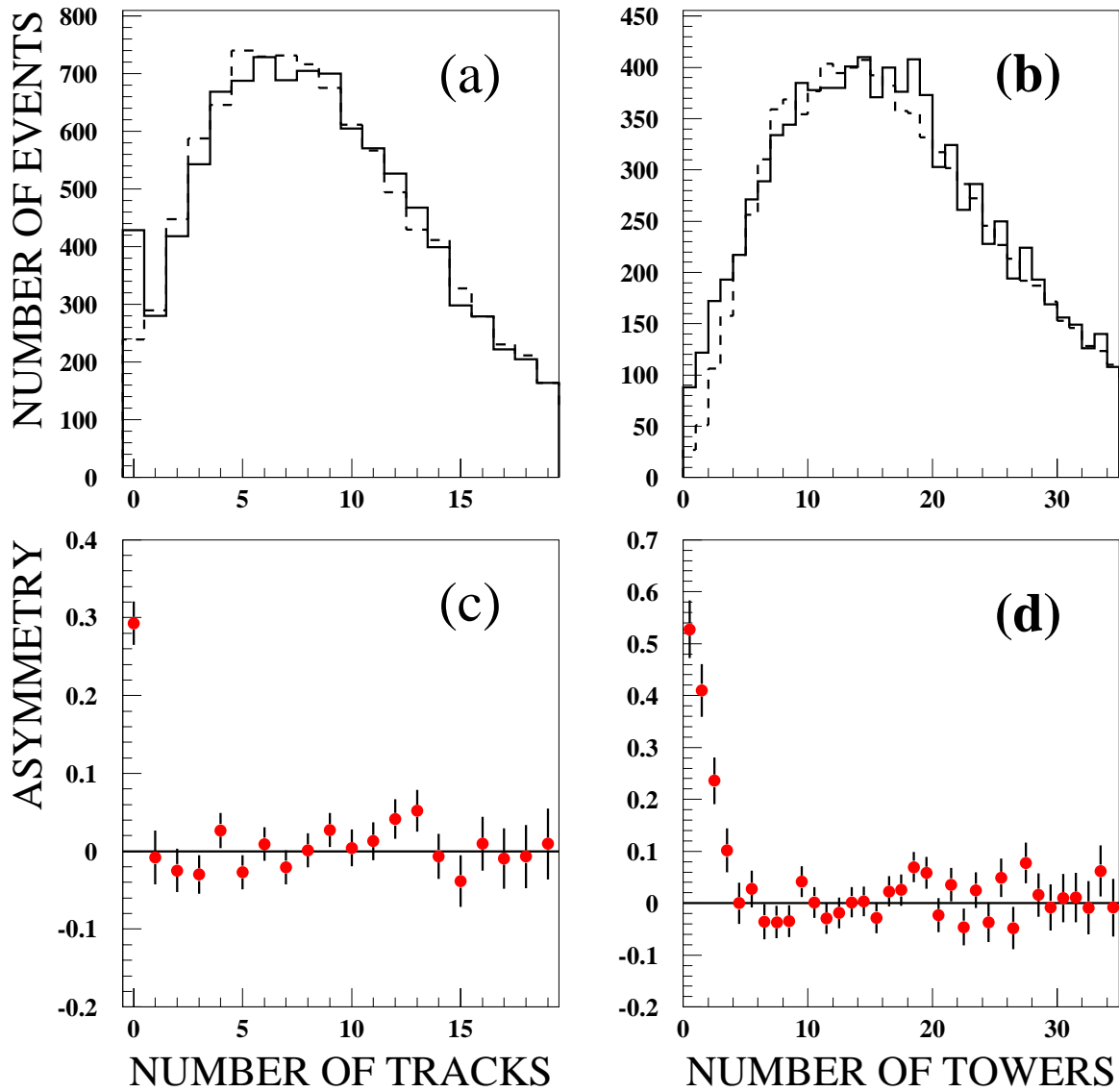


FIG. 2. Multiplicity distributions (a) for tracks with $P_T > 300$ MeV and (b) for calorimeter towers with measured $E_T > 200$ MeV in the regions $|\eta| < 1.0$ for opposite-side ($\eta_1 \eta_2 < 0$) dijet events (solid lines), and $|\eta| < 1.2$ ($|\eta| < 1.25$) for tracks (towers) of same-side ($\eta_1 \eta_2 > 0$) dijet events (dashed lines); (c,d) The bin-by-bin asymmetry, defined as the ratio of the difference over the sum of the opposite-side and same-side multiplicity distributions of (a) and (b).

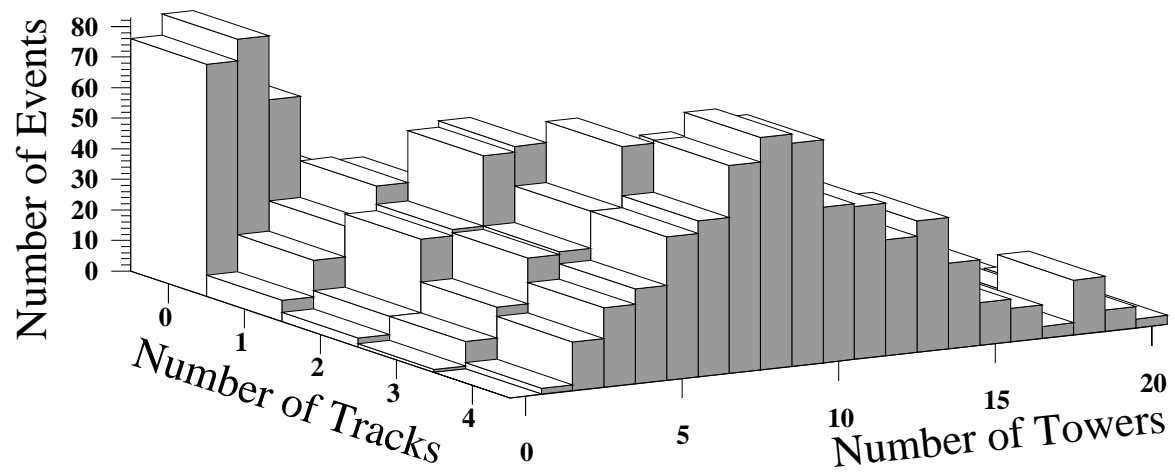


FIG. 3. Track versus tower multiplicity distribution for events in the $N_{\text{vertex}} \leq 1$ opposite-side dijet sample with $N_{\text{track}} < 5$ and $N_{\text{tower}} < 20$ within $|\eta| < 1.0$. The bins with zero tracks and 0, 1 or 2 towers contain an excess of events above the expectation from an extrapolation from the bins with $N_{\text{track}} > 1$. This excess is attributed to events from color-singlet exchange.

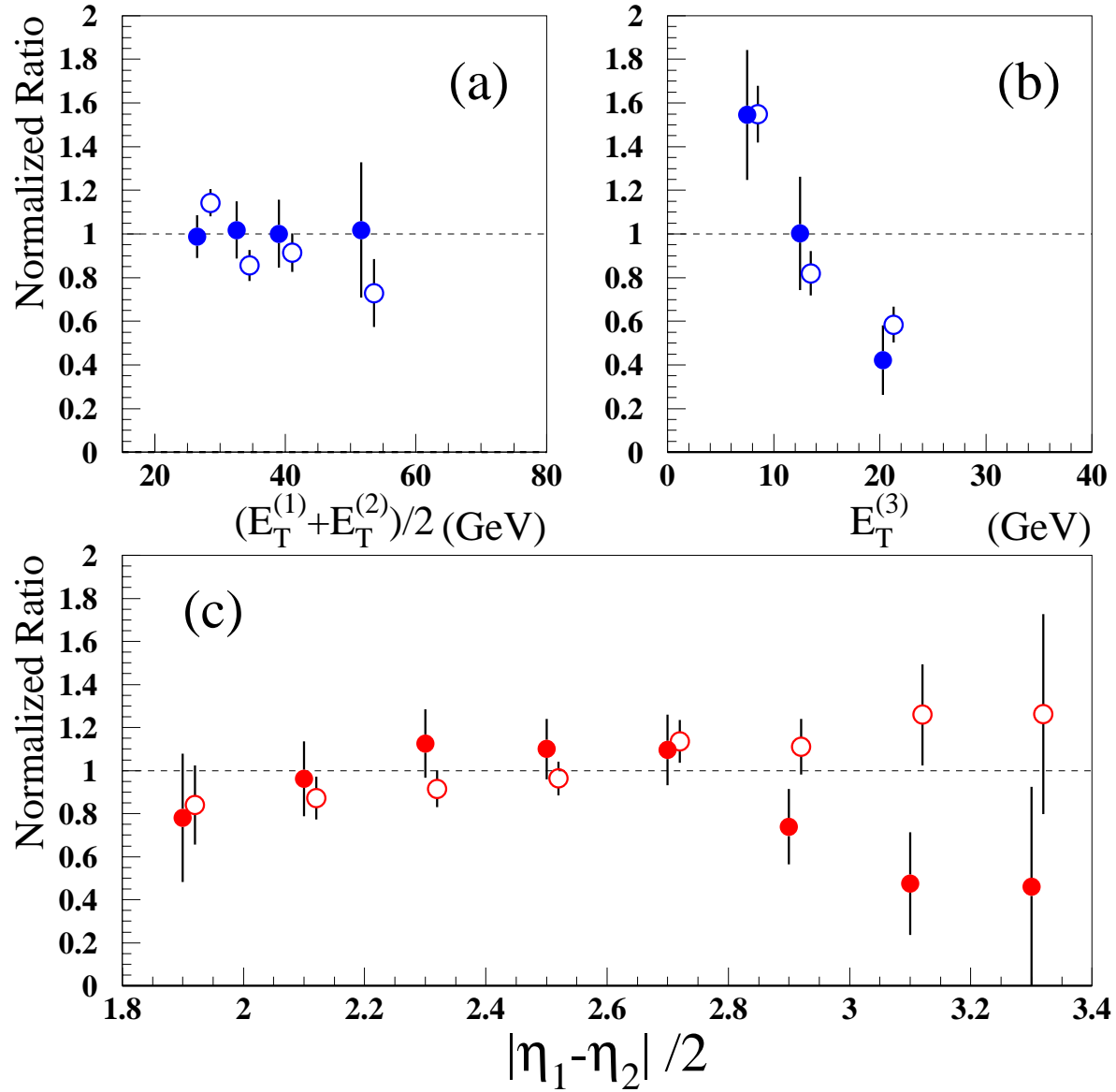


FIG. 4. Normalized (to be unity on average) ratios of gap (solid points) and control sample events (open circles) over all events versus: (a) the average E_T of the two leading jets, (b) the E_T of the third jet, and (c) half the η separation between the two leading jets.